JOURNAL OF SOLID STATE CHEMISTRY **80**, 286–298 (1989)

Structural Correlations within the Lanthanum Palladium Oxide Family

J. PAUL ATTFIELD*,† AND GÉRARD FÉREY

Laboratoire des Fluorures, UA CNRS 449, Faculté des Sciences, Université du Maine, Route de Laval, 72017 Le Mans Cédex, France

Received October 3, 1988; in revised form February 24, 1989

The recently solved structures of $La_2Pd_2O_5$ and La_4PdO_7 are described and a structure for La_2PdO_4 is proposed. These arrangements are shown to be part of a series $La_{2n}Pd_2\square_{n+2}O_{3n+2}$ formed between PdO and the *A*- or *B*-type Ln_2O_3 lanthanide oxide structures. These structures are based on a CsCl-type "LaO" lattice, with Pd inserted on cube faces, and La vacancies (□) created to stabilize the structures. Simple rules that enable these structures to be predicted are given. The *A*- and *B*-type Ln_2O_3 structures are shown to be the rhombohedrally and monoclinically distorted forms of a vacancy-ordered CsCl-type structure: $Ln_2\square O_3$. © 1989 Academic Press, Inc.

Introduction

Recently, the crystal structures of two lanthanum palladium oxdies, $La_2Pd_2O_5$ and La_4PdO_7, were solved by one of us (J.P.A.), using a simple modeling technique in conjunction with powder diffraction methods. Full details of the structure determinations are presented elsewhere (*1*). As both of these arrangements represent new structure types it is worthwhile to describe their crystal chemistry and to seek relationships between these and other structures, which is the purpose of this article.

Descriptions of Lanthanum Palladium Oxide Structures

$La_2Pd_2O_5$. The positional parameters and interatomic distances for this compound are given in Tables I and II, and the (001) projection of the structure is shown in Fig. 1. The coordinations around Pd^{2+} and La^{3+} are close to square planar and cubic, respectively. The PdO_4 square planes share all of their vertices to build up isolated "screw ladder" chains that run parallel to *c* (Fig. 2c). These are unusual in the crystal chemistry of square planar groups; the only previous instance is in the metallic conductor $CaPt_2O_4$ (*2*) in which Ca^{2+} lies between the chains (Fig. 2b). The relationship between the structures may be seen by writing their formulae as $Ca(Pt_2O_4)$ and $La_2O(Pd_2O_4)$. The insertion of additional La^{3+} and O^{2-} between the chains induces a rotation of the latter in order to maintain cubic coordination around La^{3+}. The $Na_xPt_3O_4$ (*3*) structure is derived from the $CaPt_2O_4$ structure by adding supplementary square planes which connect four ladders as shown in Fig. 2a, and so it may also be described as a three-dimensional network of interconnected ladders. The PdO struc-

* On leave from the Chemical Crystallography Laboratory, University of Oxford, 9 Parks Road, Oxford OX1 3PD, UK.

† To whom correspondence should be addressed.

0022-4596/89 $3.00

TABLE I

STRUCTURAL PARAMETERS FOR TETRAGONAL $La_2Pd_2O_5$ IN $P4_2/m$ (No. 84) WITH ESTIMATED STANDARD DEVIATIONS IN PARENTHESES

a = 6.703(2) Å c = 5.630(2) Å

Atom	Symmetry position	Fractional coordinates x	y	z
La	4(j)	0.2648(4)	0.1080(6)	0
Pd	4(j)	0.3099(6)	0.5951(6)	0
O(1)	8(k)	0.198(3)	0.402(3)	0.255(3)
O(2)	2(e)	0	0	$\frac{1}{4}$

ture (*4*) may be described as consisting of infinite, face-sharing ladders, and is further described later.

The $La_2Pd_2O_5$ structure is based on a primitive cubic sublattice of O^{2-}, in which cube centers and faces are occupied by La^{3+} and Pd^{2+}, respectively. La-filled, face-sharing double cubes are linked by edges to build up chains, as shown on the extended projection of Fig. 3. These chains run along

TABLE II

SELECTED DISTANCES (Å) AND ANGLES (°) IN $La_2Pd_2O_5$ WITH ESTIMATED STANDARD DEVIATIONS IN PARENTHESES

Bond lengths					
La–O(1)	(×2)	2.48(2)	Pd–O(1c)	(×2)	2.05(2)
La–O(1a)	(×2)	2.64(2)	Pd–O(1)	(×2)	2.07(2)
La–O(1b)	(×2)	2.69(2)			
La–O(2)	(×2)	2.378(2)			
Short *M–M* and O–O distances					
La..La(d)		3.470(6)	Pd..Pd(d)		2.850(8)
La..La(e)		3.834(6)	Pd..Pd(f)	(×4)	3.462(3)
La..La(a)	(×4)	3.908(3)	O(1)..O(1h)		2.76(3)
La..Pd(f)	(×2)	3.261(3)	O(1)..O(1i)		2.87(3)
La..Pd		3.279(6)	O(2)..O(2j)	(×2)	2.815(1)
La..Pd(g)		3.477(5)			
Angles around Pd					
O(1c)–Pd–O(1k)		84(1)	O(1i)–Pd–O(1k)		93.7(5)
O(1)–Pd–O(1i)		88(1)	O(1)–Pd–O(1k)		175.3(8)
Symmetry operation codes					
a		$y, -x, -\frac{1}{2}+z$	g		$1-x, 1-y, z$
b		$1-y, x, \frac{1}{2}-z$	h		$x, y, 1-z$
c		$y, 1-x, \frac{1}{2}-z$	i		$x, y, -z$
d		$1-x, -y, z$	j		$-y, x, \frac{1}{2}+z$
e		$-x, -y, z$	k		$x, 1-y, -\frac{1}{2}+z$
f		$1-y, x, \frac{1}{2}+z$			

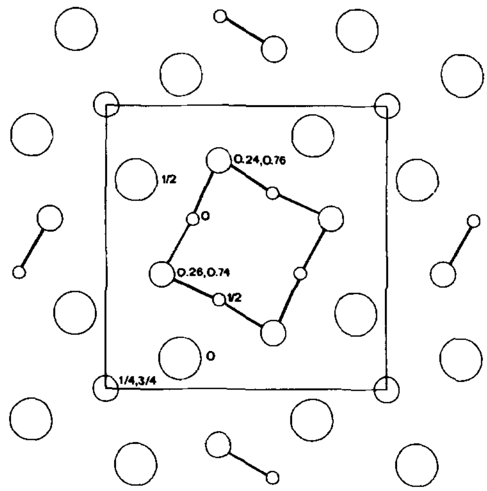

FIG. 1. The crystal structure of tetragonal $La_2Pd_2O_5$ projected on (001), with z values marked and Pd–O bonds drawn. (La/Pd/O: large/small/medium circles.)

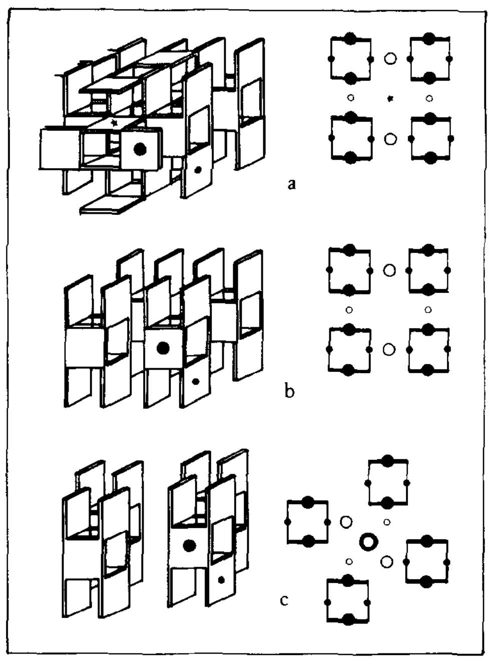

FIG. 2. Schematic and plan views of the ladders of Pd/PtO_4 square planes (Pd/Pt, filled circles) in (a) $Na_xPt_3O_4$ (additional Pt, stars; Na, circles), (b) $CaPt_2O_4$ (Ca, circles), and (c) $La_2Pd_2O_5$ (La, circles; O between ladders, double circle).

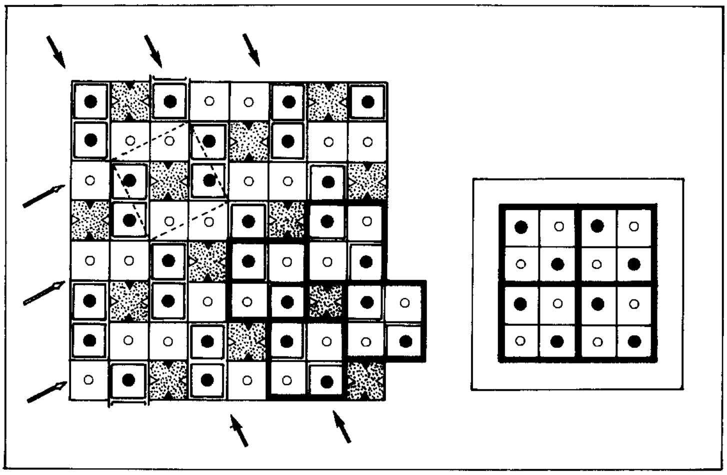

FIG. 3. An extended (001) representation of $La_2Pd_2O_5$ as a primitive cubic lattice of oxygens with the unit cell marked by dashed lines. La (circles) and Pd (triangles) occupy body and face-centering positions of the O_8 cubes, respectively. Open/filled symbols are at $z = \frac{1}{4}/\frac{3}{4}$. A similar view of the fluorite structure is shown in the insert. The cyclic shear undergone by four fluorite-like blocks is emphasized on the main figure.

[100] for z(La) = $\frac{1}{2}$ and along [010] for z(La) = 0. When the chains cross they form a basic unit of four cubes (Fig. 4) identical to that in the fluorite structure (insert of Fig. 3). Four of these blocks undergo a cyclic shear, emphasized in Fig. 3, in order to create space for the screw ladders described above. Each block contains Pd^{2+} ions on the faces of the empty cubes, as shown in Fig. 4. Face-sharing of these blocks after the cyclic shear creates the ladders (Fig. 5).

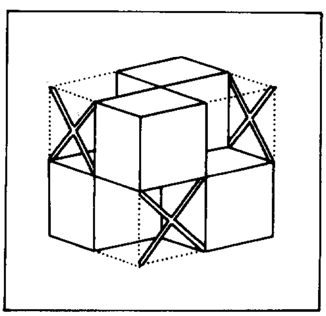

FIG. 4. A fluorite-like block in $La_2Pd_2O_5$ with the PdO_4 units emphasized. La lies at the center of the solid cubes.

La_2PdO_4. This metastable compound has not been prepared in a pure form by other workers (*5*) or ourselves. The powder pattern has been indexed on a tetragonal cell with a = 4.055 Å, c = 12.62 Å, space group *I*4/*mmm*. These data suggest that the structure is of Nd_2CuO_4 type (*6*), rather than K_2NiF_4 type, as the c/a ratio is characteristic of the former structure, but too small to be consistent with the latter (*7*), and Pd^{2+} is invariably four coordinate in metal oxides. The coordinates recently derived for Nd_2CuO_4 by neutron diffraction (*8*), shown in Table III, give a calculated X-ray diffraction pattern for La_2PdO_4 that is in good

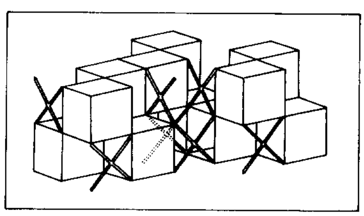

FIG. 5. The face-sharing between fluorite-like blocks (Fig. 4) in $La_2Pd_2O_5$.

TABLE III

CELL PARAMETERS,[a] PROPOSED FRACTIONAL COORDINATES,[b] AND INTERATOMIC DISTANCES FOR TETRAGONAL La_2PdO_4 IN $I4/mmm$ (NO. 139)

a = 4.055 Å c = 12.62 Å

Atom	Symmetry position	Fractional coordinates x	y	z
La	4(e)	0	0	0.351
Pd	2(a)	0	0	0
O(1)	4(c)	0	½	0
O(2)	4(d)	0	½	¼

Bond lengths (Å)

La–O(1)	(×4)	2.77	Pd–O(1)	(×4)	2.028
La–O(2)	(×4)	2.39			

Short M–M and O–O distances (Å)

La..La(a)		3.76	O(1)..O(1b)	(×4)	2.87
La..La(b)	(×4)	3.84	O(2)..O(2b)	(×4)	2.87
La..Pd(b)	(×4)	3.43			

Symmetry operation codes

a $x, y, -z$ b $\frac{1}{2}+x, \frac{1}{2}+y, \frac{1}{2}-z$

[a] Taken from Ref. (5).
[b] These coordinates were derived for Nd_2CuO_4 (8).

TABLE IV

STRUCTURAL PARAMETERS FOR La_4PdO_7 IN $C2/m$ (NO. 12) WITH ESTIMATED STANDARD DEVIATIONS IN PARENTHESES (1)

a = 13.469(1) Å; b = 4.0262(1) Å; c = 9.448(1) Å; β = 133.42(1)°

Atom	Symmetry position	Fractional coordinates x	y	z
La(1)	4(i)	0.2470(3)	½	0.1540(4)
La(2)	4(i)	0.5839(3)	0	0.3889(5)
Pd	2(a)	0	0	0
O(1)	2(b)	0	½	0
O(2)	4(i)	0.3673(4)	0	0.3101(6)
O(3)	4(i)	0.0875(5)	0	−0.1126(8)
O(4)	4(i)	0.2961(5)	½	0.4462(7)

agreement with the reported one (5) and the plausible interatomic distances shown in Table III. This structure type is again based on a primitive cubic lattice of oxide ions, and has been described elsewhere (6, 7). Infinite sheets of corner-sharing PdO_4 square planes are separated by layers of edge-sharing LaO_8 cubes.

La_4PdO_7. The crystallographic and geometric data for this structure are summarized in Tables IV and V and Fig. 6 shows the (010) projection. Isolated chains of *trans*-corner-sharing PdO_4 square planes run along b. The lattice consists of a distorted, primitive cubic network of oxide ions in which Pd^{2+} and La^{3+} occupy approximately face and body-centering positions, respectively. Considering a single layer of cubes parallel to the (201) plane, labeled I in Fig. 6, shows that La^{3+} cations are inserted to form strings of four edge-sharing LaO_8 cubes in the $y = 0$ and $y = \frac{1}{2}$ levels alternately. A shear in the (201) plane (Fig. 7) gives rise to the face-sharing of the terminal cubes from alternating chains, resulting in a ribbon of four *cis*-face-sharing cubes. The crystallographically independent La(1) and La(2) cations fill the terminal and nonterminal cubes, respectively. The stacking of these (201) layers along the [203] direction (Fig. 8) causes each $La(2)O_8$ cube to share a face with an $La(2)O_8$ cube from the ribbon in the layer above or below, and so infinite chains of *cis*-face-sharing $La(2)O_8$ cubes parallel to [203] are formed. The PdO_4 square planes lie in the (201) plane and correspond to the upper and lower faces of the O_8 cubes.

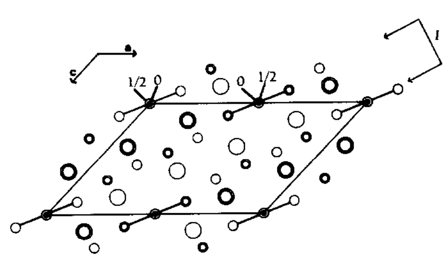

FIG. 6. A view of the ac plane of monoclinic La_4PdO_7 (La, large open circles; Pd, small filled circles; O, medium open circles) with Pd–O bonds shown. Atoms represented by single/double circles are at $y = 0/\frac{1}{2}$, except for those at (0, y, 0) and ($\frac{1}{2}$, y, 0) whose y values are labeled.

TABLE V

SELECTED DISTANCES (Å) AND ANGLES (°) IN La_4PdO_7 WITH ESTIMATED STANDARD DEVIATIONS IN PARENTHESES

		Bond lengths			
La(1)–O(1)		2.555(4)	La(2)–O(2c)		2.439(8)
La(1)–O(2)	(×2)	2.360(2)	La(2)–O(2)		2.466(7)
La(1)–O(2a)		3.510(7)	La(2)–O(3a)	(×2)	2.813(5)
La(1)–O(3a)		2.51(1)	La(2)–O(4c)	(×2)	2.373(3)
La(1)–O(3)	(×2)	2.752(4)	La(2)–O(4b)		2.517(9)
La(1)–O(4)		2.355(8)	Pd–O(1)	(×2)	2.0131(1)
La(2)–O(1b)		3.011(5)	Pd–O(3)	(×2)	2.060(9)
		Short M–M and O–O distances			
La(1)..La(1a)	(×2)	3.585(7)	La(2)..La(2d)	(×2)	3.945(7)
La(1)..La(2c)	(×2)	3.791(5)	La(2)..Pd(b)	(×2)	3.622(4)
La(1)..La(2a)		3.840(8)	O(1)..O(3)	(×4)	2.880(7)
La(1)..La(2)	(×2)	3.966(5)	O(2)..O(2c)		2.832(8)
La(1)..Pd	(×2)	3.253(3)	O(2)..O(4)	(×2)	2.884(8)
		Angles around Pd			
O(1)–Pd–O(1e)		180	O(3)–Pd–O(3f)		180
O(1)–Pd–O(3)		90			
		Symmetry operation codes			
a		$\frac{1}{2} - x, \frac{1}{2} + y, -z$	d		$\frac{3}{2} - x, \frac{1}{2} + y, 1 - z$
b		$\frac{1}{2} + x, -\frac{1}{2} + y, z$	e		$x, 1 - y, z$
c		$1 - x, y, 1 - z$	f		$-x, y, -z$

Discussion

The three lanthanum palladium oxides described above can be considered the n = 1, 2, and 4 members of the $La_{2n}Pd_2O_{3n+2}$ series. The n = 1 structure is known for $Ln_2Pd_2O_5$ (Ln = La–Gd) compounds, the n = 2 for metastable Ln_2PdO_4 (Ln = La–Dy) and Ln_2CuO_4 (Ln = Pr–Gd) (*9*), and the n = 4 structure is adopted by Ln_4PdO_7 (Ln = La–Eu) materials (*5, 10, 11*). An n = 3 compound has not been prepared with any lanthanide, and no ternary compounds have been reported in the Ln_2O_3–PdO (Ln = Ho–Lu, Y) systems at atmospheric pressure (*10*).

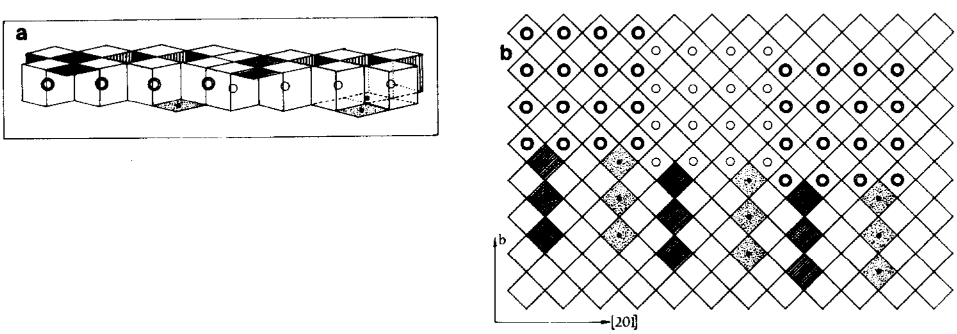

FIG. 7. (a) Perspective view and (b) plan view of a layer of O_8 cubes parallel to the (201) plane of La_4PdO_7. Single/double circles correspond to La at $y = 0/\frac{1}{2}$, and PdO_4 square planes on the upper/lower surface of the layer are hatched/speckled. In (a) vertical hatching and shading is used to emphasize the surfaces of the partially hidden La-filled cubes.

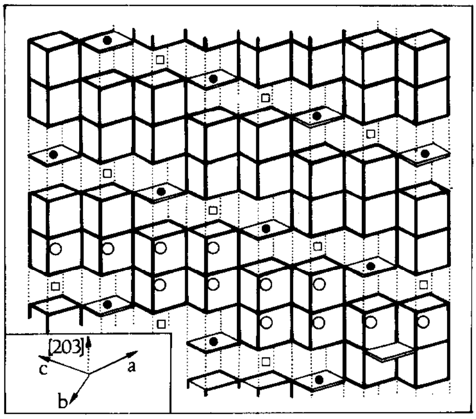

FIG. 8. The stacking of the (201) layers of cubes in La_4PdO_7 in the [203] direction (La, open circles; Pd, small filled circles). La-filled cubes are shown in bold outlines and La vacancies that are not adjacent to PdO_4 square planes are represented by squares.

The lanthanide palladium oxides are semiconductors or insulators, and the reported resistivities (*5, 11*) can be related to the linkages of square planes in their structures. Ln_4PdO_7 materials have very high resistivities ($>10^{11}$ Ω cm for Ln = La, Nd)and contain isolated one-dimensional chains with each PdO_4 unit sharing two vertices. The values for $Ln_2Pd_2O_5$ compounds are lower (4×10^6, 3.8×10^9 Ω cm for Ln = La, Nd, respectively), as the square planes share four corners to form one-dimensional ladders, and the resistivity of 4.6×10^5 Ω cm for Nd_2PdO_4 reflects the two-dimensional nature of the infinite planes of linked PdO_4 units.

Although the three lanthanide palladium oxide structures seem quite different, their structures are closely related and can be understood from two basic principles:

(1) All the structures are built up from a primitive cubic lattice of oxide ions in which Pd^{2+} and Ln^{3+} are at the face and body-centering positions of the O_8 cubes. This satisfies the requirements both of Pd^{2+} for square planar coordination and of Ln^{3+} for a high coordination number and geometric factors. The ideal ratio of bond distances $d(Ln^{3+}\text{–}O^{2-})/d(Pd^{2+}\text{–}O^{2-})$ for such structures is $\sqrt{(3/2)} \approx 1.225$, and the limiting values for Ln = La and Dy are 1.256 and 1.191, respectively, using Shannon's ionic radii (*12*). Thus the geometric requirement for compound formation is that the $d(Ln^{3+}\text{–}O^{2-})/d(Pd^{2+}\text{–}O^{2-})$ ratio has value $\sqrt{(3/2)} \pm 0.035$. No ternary lanthanide palladium oxides are observed for Ln = Ho–Lu or Y because the cations are too small. The primitive O_8 cubes have an edge length of $a_c \approx (2\sqrt{3}/3)d(Ln^{3+}\text{–}O^{2-}) \approx \sqrt{2}d(Pd^{2+}\text{–}O^{2-}) \approx 2.91$ Å for Ln = La.

(2) The cations are inserted into the oxide sublattice so as to minimize cation–cation repulsions. This means that two *cis* faces of the same cube cannot both be occupied by Pd^{2+}, although a pair of opposite faces may be. The occupation of two face-sharing cubes by Ln^{3+} is unfavorable and results in displacements of the ions so that a more favorable cation–cation distance (>3.45 Å for La^{3+}) is achieved. Occupation of the face and body-centering positions of the same cube by Pd^{2+} and Ln^{3+} is never possible.

Using these principles, all three lanthanum palladium oxide structures can be built from a CsCl-type "LaO" lattice according to a sequence of rules, by introducing La vacancies (□) and Pd according to the formula $La_{2n}Pd_2\square_{n+2}O_{3n+2}$. In the following rules, the axes of the cubic "LaO" lattice (cell parameter = a_c) are parallel to the orthogonal reference axes x_r, y_r, and z_r:

(1) Place an infinite column of LaO_8 cubes parallel to x_r and divide the column into repeat units of $3n + 2$ cubes if n is odd or $(3n + 2)/2$ cubes if n is even.

(2) Create La vacancies by placing Pd at the common face of two cubes and removing the La's from both cubes, and then, if more vacancies are required, by removing La's so as to minimize the number of shared faces per La-occupied cube.

(3) Place the columns next to each other to build up layers parallel to the $x_r y_r$ plane, with a translation of $2a_c$ in the x_r direction between successive columns at $y_r = y$ and $y_r = y + a_c$. (This minimizes face-sharing between La-occupied cubes from adjacent columns.)

(4) Stack the layers so as to minimize cation–cation repulsions, principally those due to face-sharing between LaO_8 cubes.

The repeat cation units arising from steps 1 and 2 for the $n = 1, 2$, and 4 structures are LaLa□Pd□Pd□, LaLa□Pd□, and LaLa□LaLa□Pd□, respectively. Step 3 generates the layers of cubes shown in Fig. 9a; they correspond to the actual arrangement of cations and vacancies in all three structures. However, the stacking sequence arising from step 4 is not the same for all the structures. In La_2PdO_4 and La_4PdO_7 there is a translation of a_c in the y_r direction between layers at $z_r = z$ and $z_r = z + a_c$, which completely avoids interlayer face-sharing of La-occupied cubes in the former case. In the latter structure, the cubes lying above and below each $La(1)O_8$ cube are empty, and only one of those adjacent to an $La(2)O_8$ cube is filled.

Two plausible stacking arrangements of the $x_r y_r$ layers in $La_2Pd_2O_5$ are evident. Unlike the $x_r y_r$ layers in the above two structures, those in $La_2Pd_2O_5$ have pseudofourfold axes around the centers of the vacant cubes with Pd on opposite faces, such that a 90° rotation transforms La-filled cubes into vacant ones and vice versa. Hence, a 90° rotation between successive layers allows the La^{3+} occupied cubes in one layer to lie between vacant cubes from the adjacent levels. However, the translation between layers that is observed in the $n = 2$

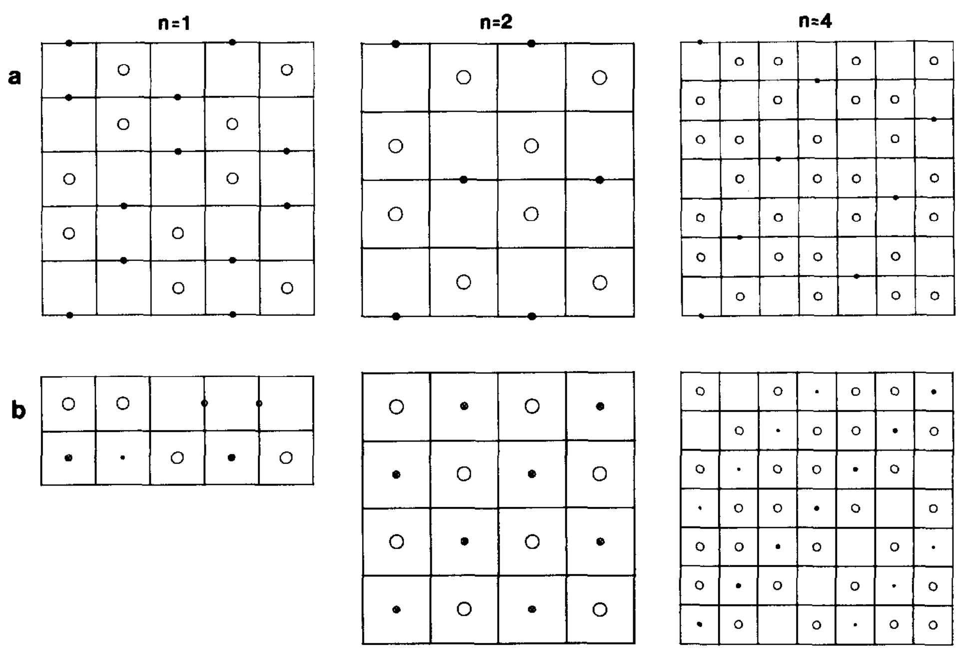

FIG. 9. The idealized $n = 1, 2$, and 4 $La_{2n}Pd_2\square_{n+2}O_{3n+2}$ structures: (a) Layers of cubes parallel to the $x_r y_r$ plane (x_r vertical, y_r horizontal); La's (large open circles) and Pd's (small shaded circles) are at $z_r = a_c/2$. (b) Layers of cubes parallel to the $y_r z_r$ plane (y_r horizontal, z_r vertical); La's (large open circles) are at $x_r = a_c/2$ and the small filled, half-filled, and very small filled circles represent Pd's at $x_r = 0$, $a_c/2$, and a_c, respectively. O's lie at all of the cube vertices.

and 4 structures also avoids interlayer face-sharing of occupied cubes, and gives rise to the same number of shared edges and vertices between LaO_8 cubes as the former operation. The favored arrangement is thus determined by considering La–Pd repulsions. The 90° rotation between successive layers results in *two* short $(\sqrt{5}/2)a_c$ distances between La and the Pd's in adjacent levels, but *three* such contacts result when there is an a_c translation between layers, and so the former operation best satisfies step 4 and gives rise to the observed structure. Figure 9b shows the layers of cubes parallel to the $y_r z_r$ plane for the three lanthanum palladium oxide structures.

Steps 3 and 4 minimize the number of face-sharing La-occupied cubes; in $La_2Pd_2O_5$ and La_2PdO_4 each LaO_8 cube shares a face with only one other. In La_4PdO_7 the occupied cubes share one or three faces, and it is notable that the vacant cube which does not have Pd on any face shares faces with six La-occupied cubes, and so presumably plays an important part in stabilizing the structure.

These operations result in tetragonal or cubic reference cells for the three structures; however, the crystallographic cell is smaller in all three cases. The transformation matrices relating the crystallographic and reference cells are given in Table VI, together with the predicted and observed cell parameters.

It is instructive to apply the above rules to consider the $n = 0$ and $n \rightarrow \infty$ composition limits.

(*i*) $n = 0$. Using the former rules to predict the structure of Pd□O gives rise to infi-

TABLE VI

TRANSFORMATION MATRICES AND CELL PARAMETERS FOR THE $n = 1, 2, 4,$ AND ∞ $Ln_{2n}Pd_2\square_{n+2}O_{3n+2}$ STRUCTURES

n	M[a]	A_r[b] (a_c)	A (a_c)	A (Å)	A_{obs} (Å)
1	$\begin{pmatrix} -\frac{2}{5} & \frac{1}{5} & 0 \\ \frac{1}{5} & \frac{2}{5} & 0 \\ 0 & 0 & -1 \end{pmatrix}$	5	$\sqrt{5}$	6.51	6.70
		5	$\sqrt{5}$		
		2	2	5.82	5.63
2	$\begin{pmatrix} 0 & \frac{1}{2} & -\frac{1}{2} \\ 0 & \frac{1}{2} & \frac{1}{2} \\ 1 & 0 & 0 \end{pmatrix}$	4	$\sqrt{2}$	4.12	4.06
		2	$\sqrt{2}$		
		2	4	11.64	12.62
4	$\begin{pmatrix} 0 & \frac{1}{2} & -\frac{1}{2} \\ 0 & \frac{1}{7} & \frac{1}{7} \\ \frac{1}{3} & \frac{1}{3} & \frac{1}{3} \end{pmatrix}$	7	$7\sqrt{2}/2$	14.40	13.47
		7	$\sqrt{2}$	4.12	4.03
		7	$7\sqrt{3}/3$	11.76	9.45
				$\beta = 145°$	133°
∞ (A)	$\begin{pmatrix} 0 & 1 & -1 \\ -1 & 0 & 1 \\ 1 & 1 & 1 \end{pmatrix}$		$\sqrt{2}$	4.12	3.93
			$\sqrt{2}$		
		3	$\sqrt{3}$	5.04	6.11
		3			
∞ (B)	$\begin{pmatrix} 1 & 1 & 0 \\ \frac{1}{3} & -\frac{1}{3} & 0 \\ 0 & 0 & -1 \end{pmatrix}$	3	$3\sqrt{2}$	12.35	14.60[c]
			$\sqrt{2}$	4.12	3.72
			3	8.73	9.28
				$\beta = 90°$	100°

[a] Matrix M performs the transformation $A = M \cdot A_r$.

[b] A_r is the column vector $\begin{pmatrix} a_r \\ b_r \\ c_r \end{pmatrix}$, etc.

[c] Cell parameters are taken from Ref. (*18*).

nite stacks of PdO_4 units in the x_r direction after steps 1 and 2 and layers of stacks that share two *trans*-edges, resulting in infinite PdO_2 chains parallel to y_r, in stage 3. For step 4 there are two possibilities, as in $La_2Pd_2O_5$. The layers can be stacked directly upon one another (as the layers are identical under the translation in the y_r direction), giving rise to infinite PdO_4 sheets, or with a 90° rotation between layers. This results in corner-sharing PdO_2 chains along y_r at $z_r = 0$, and along x_r at $z_r = a_c$, and face-sharing ladders parallel to x_r. The former operation produces an interlayer Pd–Pd distance of a_c, whereas the latter gives $\sqrt{(3/2)}a_c$, and so is the favored (and observed) structure for PdO (*4*). A view of this structure is shown in Fig. 10.

(*ii*) $n \rightarrow \infty$. The structure predicted for $La_2\square O_3$, assuming a translation of a_c between layers in step 4, is shown in Fig. 11. It is characterized by a cubic reference cell of edge length $3a_c$. Layers of infinite *cis*-face-sharing chains of LaO_8 cubes are stacked so that each cube also shares one face with a cube from an adjacent layer. This gives rise to sheets of *cis, cis, cis*-face-sharing cubes parallel to (111) in the reference coordinate system, with edge-sharing between sheets. This arrangement is in fact an idealized representation of the *A*- and *B*-type Ln_2O_3 structures.

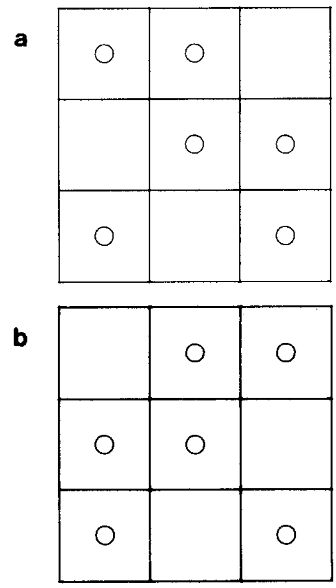

FIG. 11. (a) $x_r y_r$ and (b) $y_r z_r$ layers of the predicted $La_2\square O_3$ structure (x_r/z_r vertical, y_r horizontal), with O's at the vertices of the cubes and La's (large circles) at the body centers.

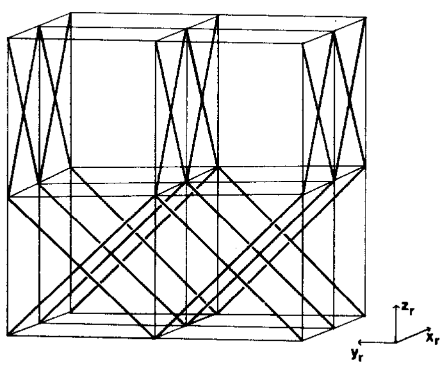

FIG. 10. A perspective view of the idealized $Pd\square O$ structure. O and Pd lie at the vertices and some of the face-centers of the cubes. Pd–O bonds are represented by heavy lines.

The relationship to the *A*-type structure may be seen by considering the layers of cations parallel to the (111) plane in the reference coordinate system of the CsCl-type "LaO" structure. Application of the above rules has resulted in every third layer of cations being removed (see Fig. 12) which

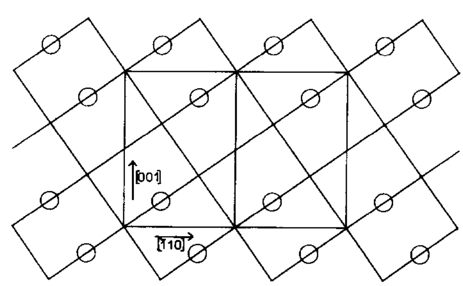

FIG. 12. The (111) projection of the $La_2\square O_3$ model shown in Fig. 11. The unit cell and crystallographic directions of the trigonal *A*-type Ln_2O_3 structure are marked.

lowers the symmetry from cubic ($Pm3m$) to trigonal ($P\bar{3}m1$). Repulsions between the remaining two cation layers gives rise to displacements of La and O(2) parallel to the unique axis such that one La–O(2) bond is elongated to 3.67 Å, and so the cation is considered to be seven coordinate. Parameters for the ideal and actual A-La_2O_3 structures (*13*) are shown in Table VII. It is interesting to note that removal of alternate layers of cations perpendicular to [111] of the CsCl structure generates the fluorite structure, and so the CsCl, CaF_2, and A-Ln_2O_3 structures may be considered the $m = 0, \frac{1}{2}$, and $\frac{1}{3}$ members of a $M_{1-m}\square_m X$ series, in which m layers of cations are removed from the CsCl structure (*14*).

An alternative unit cell for the model $La_2\square O_3$ structure is shown in Fig. 13. This has monoclinic ($C2/m$) symmetry and corresponds to the cell of the B-Ln_2O_3 structure which contains three crystallographically independent cations. The ideal and actual parameters for B-Sm_2O_3 (*15*) are shown in Table VIII. Again, the distortion of the structure due to cation–cation repulsions results in one long bond per cation with distances between 3.59 and 3.88 Å, and so the cations are considered to be only seven-coordinate.

TABLE VII

Fractional Coordinates for the Model $Ln_2\square O_3$ Structure in $P\bar{3}m1$ (No. 164)

Atom	Symmetry position	Fractional coordinates		
		x	y	z
La	2(d)	$\frac{1}{3}$	$\frac{2}{3}$	$\frac{1}{6}$ (0.2465)
O(1)	1(a)	0	0	0
O(2)	2(d)	$\frac{1}{3}$	$\frac{2}{3}$	$\frac{2}{3}$ (0.6464)

Note. The refined values for A–La_2O_3 (*13*) are also given in parentheses.

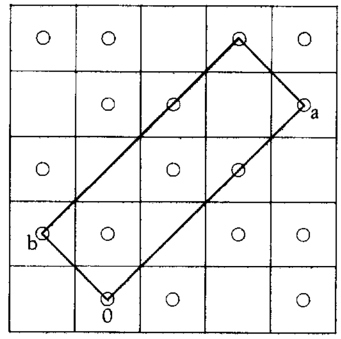

Fig. 13. An extended view of the $x_r y_r$ plane of the ideal $La_2\square O_3$ structure with the B-type Ln_2O_3 cell shown.

Hence, the A- and B-type Ln_2O_3 structures may be described as the rhombohedrally and monoclinically distorted variants of the same vacancy-ordered, CsCl-type structure.

As the rules governing the lanthanum palladium oxide structures also describe the PdO and La_2O_3 structures, the ternary phases may be regarded as ordered inter-

TABLE VIII

Fractional Coordinates for the Model $Ln_2\square O_3$ Structure in $C2/m$ (No. 12).

Atom	Symmetry position	Fractional coordinates		
		x	y	z
Sm(1)	4(i)	$\frac{2}{3}$ (0.6349)	0	$\frac{1}{2}$ (0.4905)
Sm(2)	4(i)	$\frac{2}{3}$ (0.6897)	0	$\frac{1}{6}$ (0.1380)
Sm(3)	4(i)	0 (0.9663)	0	$\frac{1}{6}$ (0.1881)
O(1)	4(i)	$\frac{1}{6}$ (0.128)	0	$\frac{1}{3}$ (0.286)
O(2)	4(i)	$\frac{5}{6}$ (0.824)	0	0 (0.027)
O(3)	4(i)	$\frac{5}{6}$ (0.799)	0	$\frac{1}{3}$ (0.374)
O(4)	4(i)	$\frac{1}{2}$ (0.469)	0	$\frac{1}{3}$ (0.344)
O(5)	4(i)	$\frac{1}{2}$	0	0

Note. The refined values for B–Sm_2O_3 (*15*) are also given in parentheses.

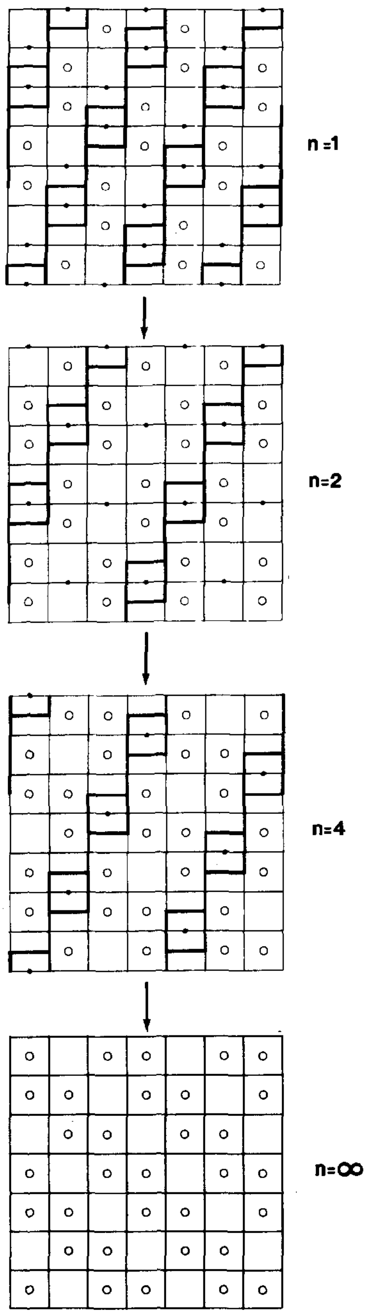

FIG. 14. A scheme showing that removal of the Pd□O units in the bold cubes along shear lines, starting from $La_2Pd_2O_5$, generates the x_ry_r layers of the n = 2, 4, and ∞ $La_{2n}Pd_2\square_{n+2}O_{3n+2}$ structures.

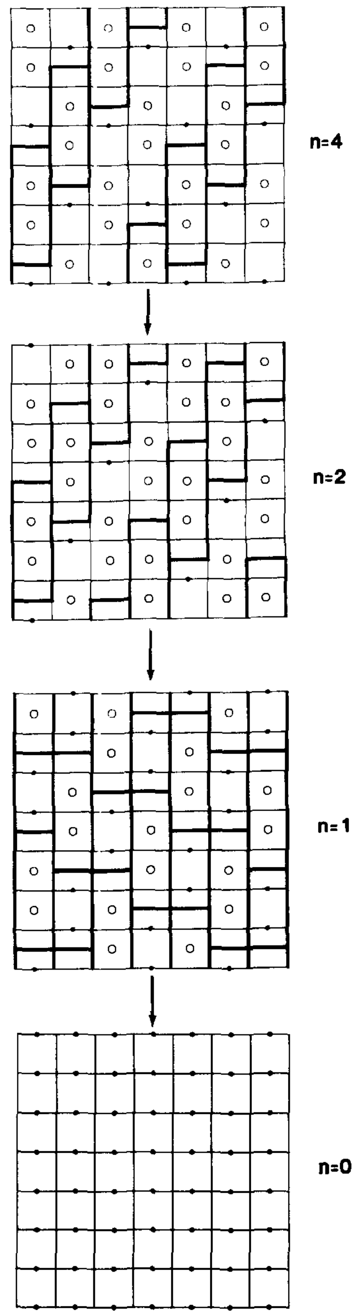

FIG. 15. Successive eliminations of $La_2\square O_3$ units (highlighted by the bold lines around three successive cubes) along shear lines, starting with La_4PdO_7, generates the x_ry_r layers of the n = 2, 1, and 0 $La_{2n}Pd_2\square_{n+2}O_{3n+2}$ structures.

growths between the two binary oxides. The general formula may then be written $(La_2\square O_3)_p(Pd\square O)_q$ and the observed structures correspond to all the possible p, q combinations for p or $q = 0$, 1, or 2.

Finally the relationships between the $x_r y_r$ layers for the five structures may be considered. Successive removals of one $Pd\square O$ per formula unit starting from the $La_2Pd_2O_5$ layer generate the higher members of the series as shown in Fig. 14. Alternatively, removals of $La_2\square O_3$ starting with La_4PdO_7 produce the layers for the structures down to $n = 0$ (Fig. 15). The $Pd\square O$ or $La_2\square O_3$ is removed along shear lines in all cases, and so the structural transformations in the two groups:

$$La_2PdO_4 \underset{-La_2O_3}{\overset{-\frac{1}{2}PdO}{\rightleftarrows}} La_4PdO_7 \xrightarrow{-PdO} La_2O_3$$

and

$$La_2Pd_2O_5 \xrightarrow{-La_2O_3} PdO$$

arise from shear planes and screw shears, respectively, as the stacking of layers within each group is the same.

Conclusions

The above arguments show that the PdO, $La_2Pd_2O_5$, La_2PdO_4, La_4PdO_7, and A- and B-Ln_2O_3 structures are the $n = 0$, 1, 2, 4, and ∞ members of an $La_{2n}Pd_2\square_{n+2}O_{3n+2}$ series. The ternary compounds may be viewed as ordered intergrowths between the two binaries, and are only known for those lanthanides which normally adopt the A- or B-type oxide structures, i.e., the La–Dy group. The B structure is stabilized for the Ho–Lu oxides under pressure (*16*), and so palladium oxides of the later lanthanides might be formed under similar conditions.

The structures are derived from CsCl-type "LaO" by placing Pd at face centers and creating La vacancies; these are important in stabilizing the structures by minimizing the number of face-sharing LaO_8 cubes. As n increases, the face-sharing of cubes increases and so the lattice becomes more distorted and the La coordination less regular. In the $n \rightarrow \infty$ limit each LaO_8 "cube" shares three faces and the model structure is distorted so that the cation sublattice becomes hexagonally close packed, and the cations are considered to be seven-coordinate (*14*). This may account for the lack of CsCl-based $La_{2n}Pd_2\square_{n+2}O_{3n+2}$ structures with $n > 4$, as the anion sublattice could not favorably accommodate both square planar Pd^{2+} and an La^{3+} sublattice that tends to distort toward close packing.

LaO (*17*) and other MO oxides of large electropositive cations adopt the cubic close-packed NaCl structure, which may be obtained by distorting the CsCl structure in the [111] direction (*14*) as a result of the cation–cation repulsions that arise in the latter arrangement. Hence, the CsCl structure is only favored for compounds containing large, polarizable, univalent metal or molecular cations.

This work illustrates the importance of cation–cation repulsions due to coulombic and short-range forces, as well as attractive cation–anion forces, in determining the crystal structures of ionic materials. This provides some chemical justification for the method based upon minimum cation–cation distances that was used to model the cation positions in $La_2Pd_2O_5$ and La_4PdO_7, from which their full crystal structures were determined (*1*).

Acknowledgments

J.P.A. thanks Christ Church, Oxford, for a Junior Research Fellowship and the Université du Maine for the position of a Maitre de Conferences.

References

1. J. P. Attfield, *Acta Crystallogr. Sect. B* **44**, 563 (1988).

2. D. Cahen, J. A. Ibers, and M. H. Muller, *Inorg. Chem.* **13,** 110 (1974).
3. J. Waser and E. D. McClanahan, *J. Chem. Phys.* **19,** 413 (1951); **20,** 199 (1952).
4. J. Wasser, H. A. Levy, and S. W. Peterson, *Acta Crystallogr.* **6,** 661 (1953).
5. B. G. Kakhan, V. B. Lazarev, and I. S. Shaplygin, *Russ. J. Inorg. Chem.* **27,** 1180 (1982).
6. H. Muller-Buschbaum and W. Wollschlager, *Z. Anorg. Allg. Chem.* **414,** 76 (1975).
7. P. Ganguly and C. N. R. Rao, *J. Solid State Chem.* **53,** 193 (1984).
8. J. Gopalkrishnan, M. A. Subramanian, C. C. Torardi, J. P. Attfield, and A. W. Sleight, *Mater. Res. Bull.,* in press.
9. H. Muller-Buschbaum, *Angew. Chem. (Engl. Transl.)* **16,** 674 (1977).
10. C. L. McDaniel and S. J. Schneider, *J. Res. Natl. Bur. Stand. Sec. A* **72**(1), 27 (1968).
11. B. G. Kakhan, V. B. Lazarev, and I. S. Shaplygin, *Russ. J. Inorg. Chem.* **27,** 2395 (1982).
12. R. D. Shannon, *Acta Crystallogr. Sect. A* **32,** 751 (1976).
13. J. P. Attfield and G. Ferey, *J. Solid State Chem.,* in press.
14. B. G. Hyde, *Acta Crystallogr. Sect. A* **27,** 617 (1971).
15. D. T. Cromer, *J. Phys. Chem.* **61,** 753 (1957).
16. A. F. Wells, "Structural Inorganic Chemistry," 4th ed., p. 450 Oxford Univ. Press (Clarendon), London (1975).
17. J. M. Leger, N. Yacoubi, and J. Loriers, *J. Solid State Chem.* **36,** 261 (1981).
18. B. Willer and M. Daire, *Bull. Soc. Fr. Mineral. Cristallogr.* **92,** 33 (1969).